The impact of land use and land cover change on hydrological processes in Brantas watershed, East Java, Indonesia

Mohamad Wawan Sujarwo[1], Indarto Indarto[*1], Marga Mandala[1],
[1]Department of Natural Resources and Environmental Management, Post-Graduate Faculty, University of Jember, Indonesia
Jl. Kalimantan No. 37 Kampus Tegalboto Jember 68121, Jawa Timur, Indonesia
*Corresponding Author: indarto.ftp@unej.ac.id

Abstract

Assessing the impact of land use and land cover change (LULCC) on hydrology is essential for water resource management. The Brantas watershed contributes about 30% of the water supply of the East Java region. The present rapid pace of land occupation for agriculture and settlements is expected to continue to alter flow processes within the watershed. This study aims to simulate LULCC and its impact on the hydrological processes of the watershed. The long-term impact of LULCC is evaluated using the Soil & Water Assessment Tool (SWAT). The analysis model is calibrated using monthly data series from 1996 to 2005 and then validated using data series from 2006 to 2015. Two editions of maps (2001 and 2015) are then used to calculate the LULCC that took place across this time period. The impacts of LULCC on hydrological processes at the sub-basin level are also evaluated. The results show that the variability of rainfall patterns from 2001 to 2015 strongly affected flow variability. The LULCC from agricultural land to other uses (irrigated rice fields, settlements and forests/plantations) is most evident in three sub-basins (sub-basins 2, 9 and 17). However, each sub-basin may respond differently with respect to the LULCC taking place. The increase in area occupied by each class of land use and cover use (LULC) is not always linear to the observed flow, and widely differing LULC classes may display similar flow responses while classes with similar characteristics may have differing impacts on flows within a sub-basin. In other words, the hydrological processes taking place are too complex to be simplified at the sub-basin level.

Keywords: LULC change; climate change; monthly flow; SWAT.

1. Introduction

Climate change (CC) and land use and land cover change (LULCC) may generate complex hydro-environmental problems at both global and local levels. Both CC and LULCC may represent changes propagated by human-induced activities (IPCC, 2007; Parece & Campbell, 2015). When both affect the same area, the impact of the two phenomena (CC and LULCC) may propagate severe hydro-meteorological disasters such as flash floods and landslides (as detailed in the works of Spruce *et al.*, 2018; Lamichhane & Shakya, 2019).

There are many possible drivers of LULCC. It may be caused by aspects of rapid development of urbanisation, such as urban sprawl, peri-urban migration, and conversion of agricultural land to pavemented areas. Furthermore, industrial sites, transportation networks, education and cultural facilities, agricultural sites, and tourism activities may all contribute to change. However, actual change may be caused by a combination of types of development (Al-Jiboori *et al*., 2020; Ahmed & Alla, 2019).

Researchers usually study LULCC by investigating two or more maps produced at different times, for example, the work of Ptak & Ławniczak, 2012; Marie Mireille *et al.,* 2019). Conventional

1

maps and satellite images can be interpreted to study the causal effects of LULCCs and their implications for society and the environment (Kang *et al.*, 2019). The use of Landsat imagery to study LULCC is a widely known method and has been published in research reports worldwide (e.g. Lamichhane & Shakya, 2019; Marie Mireille *et al.*, 2019; Li *et al.*, 2019; Al-Jiboori *et al.*, 2020). LULCC may have positive and/or negative impacts on hydrological processes. However, human activities tend to change the natural landscape into human-influenced landscapes that have the potential to disturb natural processes.

Other research has investigated LULCC related to CC processes and the various impacts caused. Ermoshin *et al.* (2013) studied long-term land use change in the transboundary Amur river basin. Nikitin *et al.* (2019) have evaluated the possible impact of LULCC in the central part of the East European plain on regional meteorological conditions using the regional COSMO model. CC and LULCC are the main drivers of streamflow change and play predominant roles both upstream and downstream (Liu *et al.*, 2020). The effects of CC and LULCC on hydrological processes have been discussed extensively by Kang *et al.*, 2019 and Liu *et al.*, 2020. The impacts of LULCC on hydrological processes are usually elaborated using a hydrological model. For example, Liu *et al.* (2020) use the Distributed Hydrology Soil Vegetation Model (DHSVM) for their study of the Beichuan river basin in the northeast Tibetan plateau.

The SWAT (Soil & Water Assessment Tool) is frequently used to simulate the impact of LULCC on hydrological processes (Arnold *et al.*, 2012). SWAT can analyse the impacts of climate, soil, vegetation and agricultural activities on river flow, and researchers worldwide have used it to study the impact of LULCC and CC on hydrological processes, for example the work carried out by Lamichhane and Shakya (2019) in Nepal. A similar study has been conducted by Mireille *et al.* (2019) in Kenya, and Kang *et al.* (2019) have applied SWAT and statistical methods to evaluate the effects of climate and land use change on surface hydrology in the Loess Plateau hilly-gully region of China.

Recently, Li *et al.* (2019) have applied the SWAT model to the analysis of LULCC and CC impacts. They state that decrease in forest, grass and wetland areas has reduced water balance and baseflow, but that annual evapotranspiration has increased. Finally, Rafiei *et al.* (2020) have used SWAT to identify soil erosion hotspots through simulating hydrological processes, soil erosion and sediment transport. The SWAT model is based on the concept of the hydrological response unit (HRU) used to calculate spatially distributed hydrological processes (Arnold *et al.*, 2012). The HRU approach dynamically analyses and models the hydrology of various structures into homogeneous structures based on their soil type, geology, and cover-crop interactions. Each HRU will produce one hydrological value distributed to other HRUs based on land cover, soil and slope (Pignotti *et al.*, 2017). The hydrological processes identified influence vegetation growth, and determine nutrient, pesticide and sediment movements within the watershed. The vertical components of water balance are calculated for each HRU and then the runoff, sediments and nutrients are accumulated from the HRUs to each sub-basin. The horizontal movement of water, nutrients and sediments from each sub-basin to the watershed outlet is then calculated using the transfer function (Arnold *et al.*, 2012).

This research aims to use the SWAT model to simulate LULCC during two ten-year periods between 1996 and 2015 and to elaborate on their impact on hydrological processes as modelled at the monthly level. The study is conducted in Brantas watershed in East Java Province, Indonesia.

2. Materials and Methods

2.1 Study area

Brantas watershed (Figure 1) covers an area of 14,103 km^2, equivalent to 30% of East Java Province's total area (47,075.35 km^2). The length of the main channel of the Brantas river is 320 km. The Brantas watershed area includes the administrative districts and cities of Malang, Kediri, Blitar, Nganjuk, Batu, Blitar, Tulungangung, Trenggalek, Jombang, Mojokerto, Sidoardjo and Surabaya (Table 1). This study focuses on the upstream and middle regions of the watershed
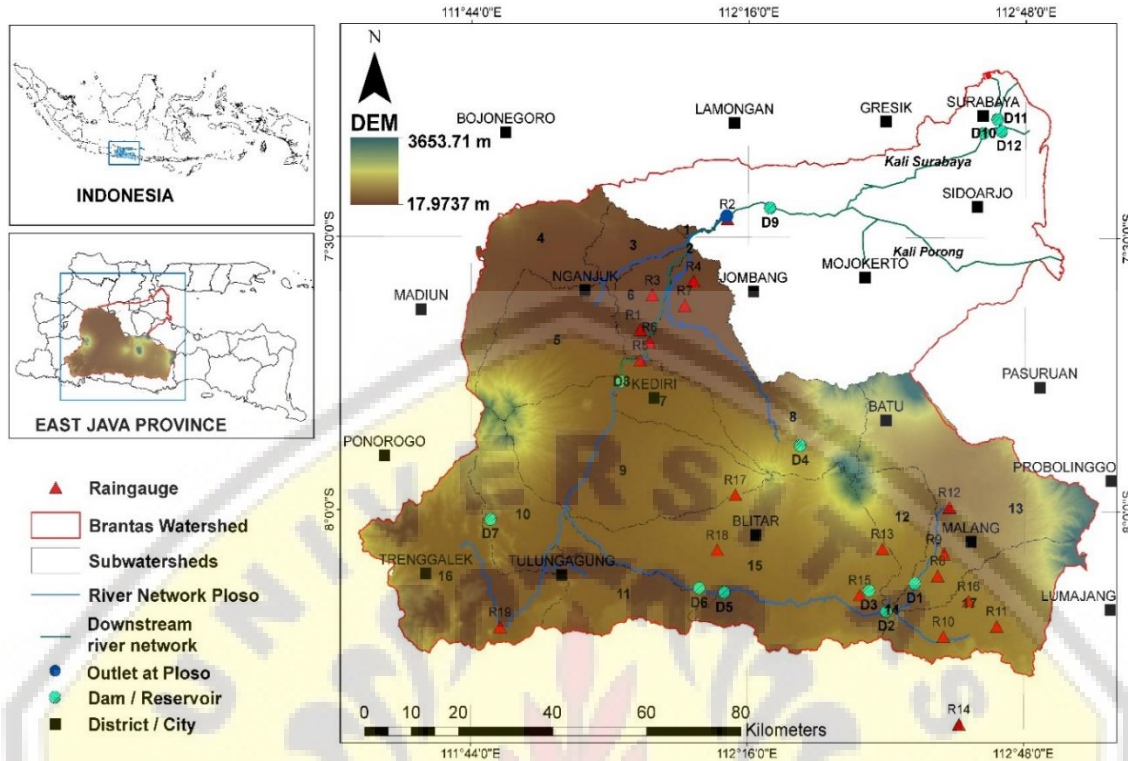
Fig. 1 Study area

(8842.76 km^2). The watershed area is populated by more than 8 million inhabitants (> 30% of the population of East Java) (BPS Jatim, 2017) and is the most urbanised area in the region (Table 1). The land is occupied for residential use, agricultural land, urban and city facilities, road networks, tourism sites, plantations, industry, and other social–cultural economic activities.

Table 1. District and city administrative areas in the Brantas watershed (Source: BPS Jatim, 2017)

District/city	Area (Km^2)	Population (in 1000s)		Population (%)
		2000	2015	
Batu	189.54	168	200	19.0
Blitar District	1299.74	1065	1145	7.5
Blitar City	33.35	119	137	15.1
Bojonegoro	2.13	1165	1236	6.1
Jombang	276.4	1127	1241	10.1
Kediri District	1485.79	1408	1547	9.9
Kediri City	69.14	245	280	14.3
Lamongan	0.03	1182	1188	0.5

Lumajang	3.79	965	1030	6.7
Madiun	127.85	640	676	5.6
Malang District	2257.5	2244	2544	13.4
Malang City	109.95	757	851	12.4
Mojokerto	0.82	908	1080	18.9
Nganjuk	1284.3	973	1042	7.1
Pasuruan	6.1	1367	1582	15.7
Ponorogo	71.08	841	867	3.1
Probolinggo	0.13	1005	1140	13.4
Trenggalek	643.96	650	689	6.0
Tulungagung	981.12	930	1021	9.8
Total population	8842.76	17,759	19,496	194.6

About 60% of the agricultural produce of the province comes from areas served by tributaries of the Brantas. Major reservoirs for collecting water have been constructed on these tributaries: D1 (Sengguruh), D2

3

(Sutami), D3 (Lahor), D4 (Selorejo), D5 (Lodoyo), D6 (Wlingi), D7 (Wonrorejo), D8 (Waru Turi), D9 (Menturus), D10 (Gunungsari), D11 (Gubeng), and D12 (Jagir Dams) (Fig. 1).

The population of East Java increased from 34 million in 2000 to more than 39 million in 2019, an increase of 16.76% (more than 5.6 million people). Thus, the watershed plays a vital role in shaping the limits and capacity of the environment to support this region's sustainable development.

The rapid development of population, urbanisation, industrial sites, food services, energy and tourism has significantly converted natural landscapes to human-influenced ones over the last two decades, and this has led to changes in the hydrological regime of the river.

These changes are likely to exacerbate the risk of erosion, sedimentation and landslides in coming years. Land cover changes in the Brantas watershed have already had an impact on erosion and flooding, with about 70% of the eroded area being categorised as having suffered severe erosion and being prone to flooding (DLH Jatim, 2017).

Other water resource management problems in the watershed include a lack of availability of water for irrigation and water supply, below standard water quality, the presence of domestic waste in the river body and irrigation channels, rapid erosion, and sedimentation processes. The risk of flood and drought events has also increased (Anwar & Kusumawati,2015; Indarto *et al.*, 2020).

2.2 Input data

This study used flow measurements located in Ploso. Then, the sub-watershed boundary was delineated using Ploso as an outlet. The sub-watershed area covers an area of 8,844.26 km^2 (Figure 1).

The inputs to SWAT are digital elevation model (DEM) data, land cover, soil characteristics, climate variables (rainfall, temperature, solar radiation, relative wind speed and humidity), and land management practices. All of the input spatial data are formatted in a raster graphic (Table 2). In this study, ArcSWAT (2012) is used as the primary tool for hydrological analysis, while GIS software visualises the maps.

Table 2. Description of model inputs

Data type	Source	Description
DEM (digital elevation model)	Geospatial Information Agency of Indonesia (BIG, 2019)	Resolution 8.3 m
Digital soil layer	Soil Research Institute, 1998, Bogor, Indonesia	Scale 1:250000
Land use–land cover layer	Rupa Bumi, Indonesia https://tanahair.indonesia.go.id/) Intepretation of Landsat 8	Scale 1:250000 (satellite image)
Climate/	Meteorology and Climatology	1996–2015 (20 years)

4

Meteorological data series	Geophysical Agency of Banyuwangi	
Daily rainfall data	19 measurement sites (R1 to R19, as in Fig.1)	1996–2015 (20 years)

2.3 Procedure

The general modelling procedure consists of four steps as illustrated in Figure 2: (1) watershed delineation and development of HRU; (2) modelling with SWAT, including table creation, climate data input and model output into SWAT; (3) calibration and validation; (4) simulation of the impact of LULCC on hydrology.
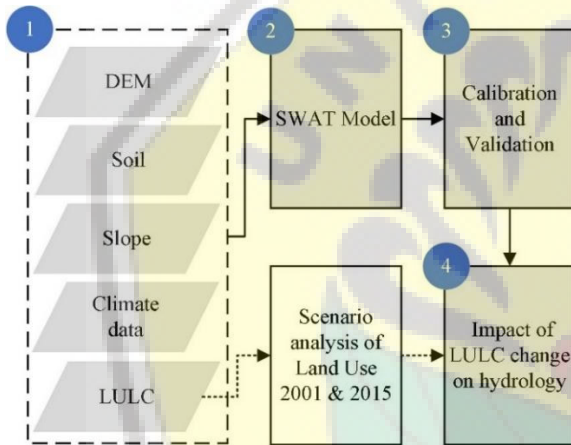

Fig. 2 Procedure

1. Watershed delineation and HRU processing: The ArcSWAT module fills sinks to determine the input DEM flow direction and accumulation (BIG, 2019). The result is then used to create the stream network, outlet and sub-basins. ArcSWAT will delineate the boundary of the watershed and produce the HRUs. HRUs are constructed from three layers: LULC maps, soil-type maps and slope classes. Finally, each HRU is determined using a 10% threshold.

2. In the SWAT model, the SWAT weather database (Weather Generator) calculates 14 necessary parameters. Seven parameters depend on rainfall data, and the other seven are adjusted for climate data (Table 2). The parameters are then used for updating to the SWAT database (SWAT Output).

3. Calibration is set for the ten-year period 1996 to 2005, while validation is for the period 2006 to 2015. The model is tested for the two periods using the SWAT graphical user interface (GUI). Simulation results are then read through the SWAT output menu. The SWAT CUP module is used to evaluate model performance. In this case, SUFI-2 (Sequential Uncertainty Fitting) is explored to fit the parameter values during calibration and validation. Calibration and validation follow the procedure as published by Abbaspour (2015). Water balance is calculated for monthly and annual intervals. Sensitivity analysis is then conducted by following procedures used in previous publications (Arnold *et al.*, 2012; Moreira *et al.*, 2018; Brighenti *et al.*, 2019). About 33 parameters are selected for sensitivity analysis and then 500 iterations are run in the model. In this case, the *r* (multiples) and *v* (replace) procedures are used to find optimal parameter values (Abbaspour, 2015). Two statistical tests are used to evaluate model performance: the Nash-Sutcliffe Efficiency (NSE) test and coefficient of determination (R^2) (Moriasi *et al.*, 2007).

4. Water balance, water, and sediment yield are then calculated during the simulation periods to enable study of the impact of LULCC on hydrology.

3. Results and Discussion

3.1 Land use/land cover change (LULCC)

This study covers the period from 1996 to 2015. Two map editions of land use (LU) and land cover (LC) are used for this study (Figure 3).
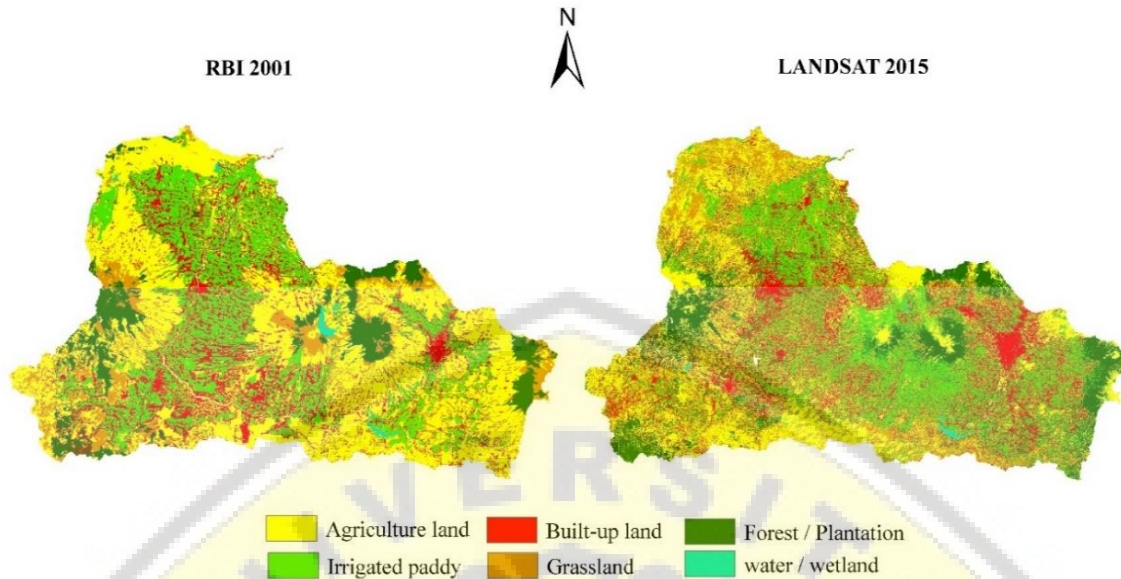
Fig. 3 LULC maps for 2001 and 2015.

The first is an LULC map clip from RBI digital maps (BIG, 2019). The RBI map was produced during the year 2000–2001. The second map clip is from classified Landsat-8 images. The available time series data are divided into periods 1 (1996–2005) and 2 (2006–2015) and the model was run for these periods. The RBI data represents LULC for the first period, while Landsat data represents LULC for the second period (Figure 3).

LULCC in the Brantas watershed from 2001 to 2015 is significant. The change is marked by increasing irrigated paddy (+ 8.4%) and forest/plantation areas (+ 4.7%). The land occupied by built-up areas also increased by + 6.5%. These increases are compensated for by a 20.6% decrease in agricultural land (non-irrigated areas) (Table 3).

Table 3. LULC in the Brantas watershed

LULC	Area (%)		Change (%)
	2001	2015	
Irrigated paddy	24.7	33.1	8.4
Agricultural land	43.4	22.8	-20.6
Built-up land	16.4	22.9	6.5
Grassland	6.7	7.8	1.0
Forest/plantation	8.2	12.9	4.7
water/wetland	0.5	0.6	0.1

Reduction in vegetation coverage will increase water flow and cause curve number values to increase. Canopy and plant root systems influence the hydrological function of the watershed, especially in relation to runoff and baseflow.

3.2 Calibration and validation

As listed in Table 4, parameters values are evaluated through iteration processes on the SWAT CUP module. Table 4 shows the best-fitted results for parameter values. The *t*-stat value indicates the sensitivity of the parameter, with *t*-stat value of 0 indicating the most sensitive parameter.

Furthermore, the *P*-value of a parameter visualises how its strength contributes to the flow calculation. *P*-value close to 1 signifies the most strongly determinant parameter, and therefore the change in calculated flow is made more significant by changing or manipulating this parameter's value (Abbaspour, 2015).

Finally, Table 4 presents the fitted values of the nine parameters most sensitive to producing runoff for the Ploso. Data in Table 4 is obtained after 10 x simulation processes and is treated with 500 iterations for each simulation (Brighenti *et al*., 2019).

Figure 5 then presents the observed and calculated hydrograph of monthly flow for calibration

6

periods from 1996 to 2005. The calibration processes produce NSE = 0.66 and R² = 0.67. The calculated flow pattern follows the fluctuation of observed flow and rainfall events. The validation processes then produce NSE and R^2 of 0.55 and 0.56, respectively.

Table 4. The fitted value of each parameter

Rank	Parameter name	Definition	*t*-stat	*P*-value	Fit
1	V__GW_REVAP.gw	Groundwater revap coefficient	0.16	0.87	0.06
2	V__ESCO.hru	Plant uptake compensation factor	-0.19	0.85	0.13
3	V__SMFMX.bsn	Maximum melt rate for snow during the year (occurs on the summer solstice)	-0.26	0.80	15.09
4	R__SOL_AWC.sol	Available water capacity of the soil layer (mm H$_2$O/mm soil)	-0.26	0.79	1.03
5	R__SLSUBBSN.hru	Average slope length (m)	-0.27	0.79	22.25
6	R__CH_N1.sub	Manning's *n* value for the tributary channels	0.35	0.73	1.31
7	V__GW_DELAY.gw	Groundwater delay (days)	-0.37	0.72	0.57
8	R__CH_L1.sub	The longest tributary channel length in the sub-basin	0.38	0.70	87.93
9	V__REVAPMN.gw	Threshold depth of water in the shallow aquifer for revamp to occur (mm)	-0.43	0.67	66.90
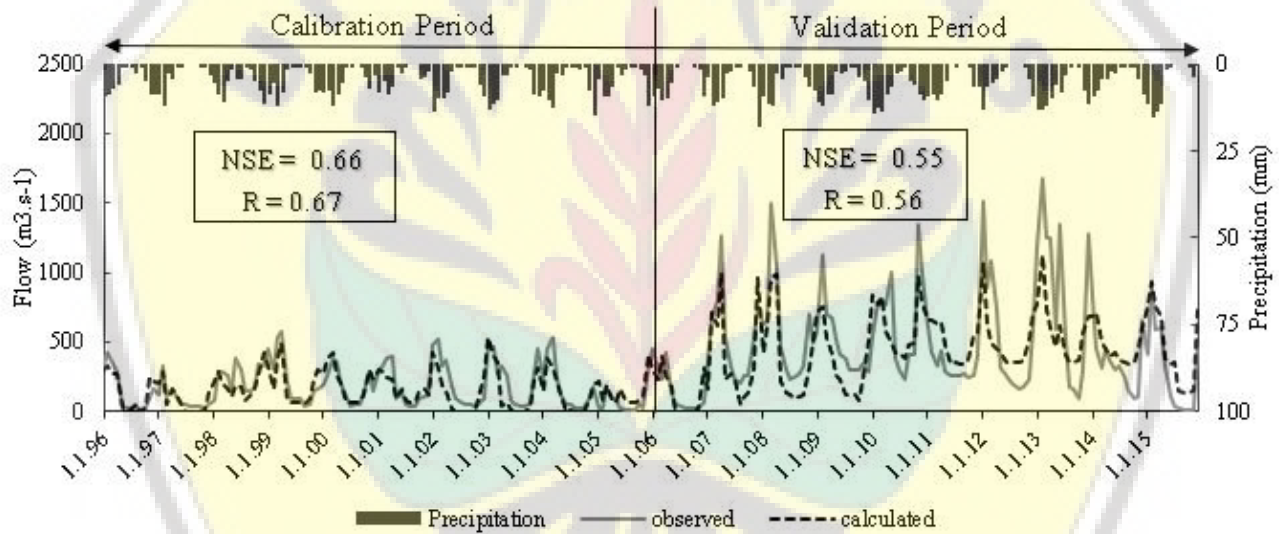
Fig 4. Monthly calculated and observed flow (1996–2015).

3.3 Water yield

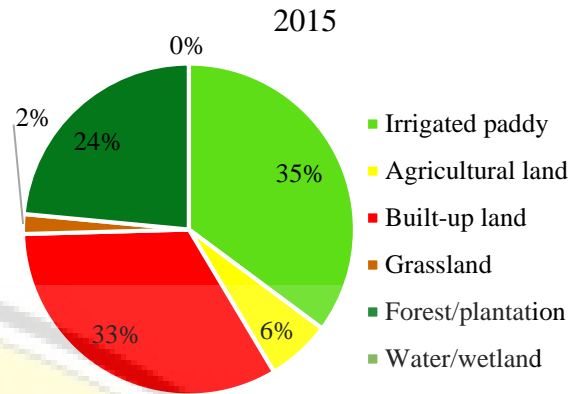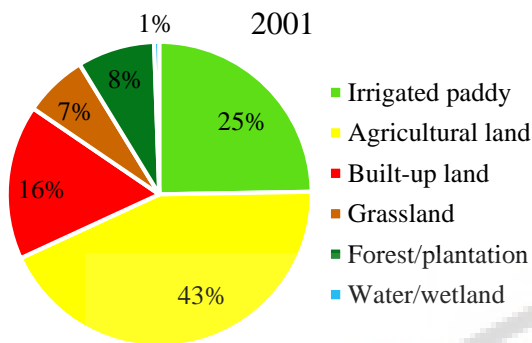Figure 5 presents the LULC of the watershed produced from clips from RBI (2001) and Landsat (2015).
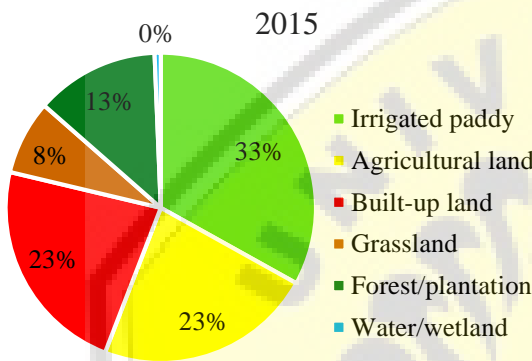
7

Fig. 5. LULC 2001 and 2015

Fig. 6. Water yield 2001 and 2015.

A significant change has occurred in four classes of land use: agricultural land, irrigated paddy, built-up land and forest. These four classes cover about 92% of the total area. In 2001, 43% of the watershed area was occupied by agricultural land (Figure 5: top image) and this produced 65% of the total water yield in the same year (Figure 6: top image).

It can be seen that 43% of the watershed area is cultivated for varied agricultural products such as corn, carrots, and many types of legume. A further area (± 25% of the total) is used for irrigated paddy.

The water yields shown in Fig. 6 are calculated for each LULC class. Agricultural practices, when they become dominant as land occupations, will produce more and more runoff. Therefore, 43% of agricultural land produces 65% of the total water yield in 2001. Usually, agricultural land is cultivated from the late wet season (monsoon) until the dry season. The crops typically have low coverage compared to grass land, and their roots occupy only the soil's upper layer. Fig. 7 presents a view of a typical seasonal crop cultivated around annual trees. The bare soil in the photo represents crop replacement after harvesting.
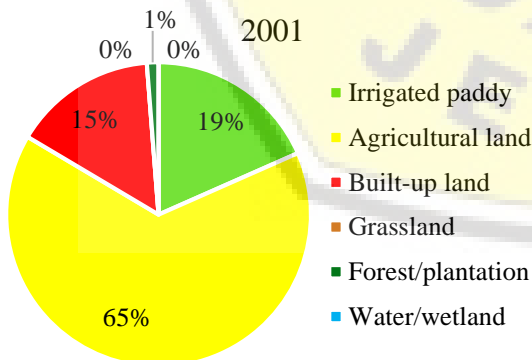

Fig. 7 Example of agricultural practice in the steepest hilly terrain.

8

Moreover, most crops are cultivated in hilly areas with the steepest slopes in the terrain. As a result, less water will be saved in the soil layer, tending to produce more runoff when precipitation falls (Fig. 7). In the year 2015, LULC has changed significantly. More agricultural land has been converted to irrigated paddy. This change results from the increase in available water supply for irrigation and a new irrigation network (Fitri *et al.*, 2017; Valiant *et al.*, 2021).

The percentage of the land occupied by built-up areas and forest/plantation is also more significant in 2015 than in 2001. The water yield in 2015 is therefore more marked in irrigated paddy, built-up areas, and forest/plantation areas. The impact of LULCC on water yield is determined by the proportion of LULC classes in watershed areas. However, this process results from many sub-processes and is moderated by type of LULC, soil, topography and climate change.

3.4 Overall watershed area

Table 5 show the annual water balance components of the whole area of the watershed: precipitation (P), water storage in soil profile (SW), actual evapotranspiration (ET), potential evapotranspiration (PET), water yield (WY) and sediment yield (SY). The water balance is calculated using two LULC scenarios: the LULC map for 2001 calculates the water balance using data from from 1996 to 2005,

while the LULC map for 2015 uses data for 2006 to 2015.

In general, all hydrological components increase in the second period (2006 to 2015): P increases to 16.6%, SW increases to 296.7%, PET to 2.4%, WY to 26.2%, and SY to 68.7%. At the same time, the ET component decreased to 29.6%. The decrease in ET reflects the fact that the vegetation coverage was less in the second period than in the first period (1996 to 2005).

However, the annual water yield (WY) and sediment yield (SY) values varied from year to year. For example, in the first period of 1996 to 2005, in wet years (years with high rainfall events such as 1998–2001) the annual WY and SY values are more important than in dry years (such as 1996–1997). The period 1996–1997 was an intense El Nino period, in which the East Java area was the driest. It is shown that rainfall, as an element of CC, still more strongly influences hydrological processes than the LULCC.

Table 5. Comparison of annual hydrologic features

Scenario of land use 2001						Scenario of land use 2015					
year	P	SW	ET	PET	WY	SY	year	P	SW	ET	PET	WY	SY
1996	1570.7	7.5	502.0	1952.1	1141.6	946.1	2006	1237.2	54.3	256.6	1852.1	953.6	368.9
1997	1158.7	8.1	426.7	2194.3	724.7	385.1	2007	1905.3	86.0	354.5	2027.5	1431.2	727.8
1998	3990.6	20.9	606.8	1881.4	3344.4	1959.0	2008	1714.3	76.7	335.8	2007.1	1388.1	597.0
1999	3736.6	19.4	513.0	1797.1	3198.0	1794.8	2009	1945.3	84.0	405.7	2151.7	1486.8	573.0
2000	3923.1	10.9	548.7	1751.2	3361.4	2202.4	2010	4267.5	63.5	403.7	1787.3	3818.3	3238.1
2001	3680.1	13.3	535.5	1925.7	3120.8	1998.9	2011	3789.1	62.4	334.8	1875.4	3445.9	3789.2
2002	1632.5	22.5	554.6	2156.3	1067.3	1115.3	2012	3778.8	62.9	327.4	1775.2	3414.7	3734.5
2003	1825.3	31.5	494.4	1953.7	1322.8	1066.8	2013	4145.1	61.9	379.1	1941.3	3738.8	3665.3
2004	879.3	12.5	282.6	2036.6	616.5	588.4	2014	3726.8	61.7	359.1	2111.1	3345.9	3765.6
2005	3741.6	23.7	522.9	1920.6	3186.3	2534.1	2015	3970.5	62.1	354.3	2508.3	3579.1	4149.6

9

| Avg | 2613.9 | 17.0 | 498.7 | 1956.9 | 2108.4 | 1459.1 | Avg | 3048.0 | 67.6 | 351.1 | 2003.7 | 2660.2 | 2460.9 |

P = precipitation (mm), SW = water storage in soil profile (mm), ET = actual evapotranspiration (mm), PET = potential evapotranspiration (mm), WY = water yield (mm), SY= sediment yield (ton/ha), Avg = average.

3.5 Impact at sub-watershed scale

The three sub-basins (2, 9 and 17) detailed in Table 6 were selected to track the impact of LULC and flow changes. In sub-basin 2, increase in grassland and decrease in irrigated paddy and agricultural land areas contributed to the rise in SW by 57.9 mm. In contrast, ET reduced to 221.1 mm. Consequently, WY increased to 1832.9 mm (+ 768.3 mm from 2001 to 2015). In sub-basin 9, decrease in irrigated paddy, agriculture and grassland and increase in forest/plantation and built-up land led to reduction in ET by 131.7 mm and contrasting impact on increase in SW and WY of 69.6 and 508 mm, respectively.

Table 6. Comparison of annual hydrologic features

Sub-basin	2		9		17	
LULC	2001	2015	2001	2015	2001	2015
Area km^2	2.2	2.2	978.9	978.9	596.9	596.9
Irrigated paddy %	64.4	41.2	34.2	29.5	11.1	35.3
Agricultural land %	24.4	21.4	34.7	27.8	64.8	16.4
Built-up land %	10.4	15.7	19.8	27.4	12.7	21.2
Grassland %	0.0	9.3	5.9	3.4	3.0	6.2
Forest/plantation %	0.0	0.0	5.0	11.6	8.5	20.7
Water/wetland %	0.0	12.2	0.0	0.2	0.2	0.1
P mm	1596.7	2239.8	1435.9	1862.6	36,243.9	36,142.4
PET mm	1904.6	2496.3	1917.3	2502.9	1934.3	2484.1
ET mm	527.0	305.9	504.8	373.1	1510.0	897.7
SW mm	3.1	61.5	10.5	80.1	62.1	89.0
WY mm	1064.3	1832.9	919.7	1427.7	34,423.0	35,190.1

Moreover, in sub-basin 17, an increase in built-up land, irrigated paddy, forest/plantation and agricultural land impacted on rise in SW and PET, producing a decrease in ET. The change of LULC class areas is not purely linear to the change in hydrological response. Different LULC combinations can have similar hydrological effects while similar LULC combinations can yield different hydrological responses. Many factors may contribute to the processes detailed above, such as intensity and distribution of rainfall and topography (Lu *et al.*, 2015). In reality, the hydrological response observed in the sub-basin level and the whole watershed areas is more determined by the simultaneous and combined effect of changes (CC and LULC).

4. Conclusion

This study concludes that changes in LULC from 2001 to 2015 included the transformation of agricultural land into irrigated rice fields, settlements and forests/plantations. These changes reflect increased socio-economic development (irrigation water services, population, and plantation potential) in the East Java region. Three types of LC contributed most to water yield (WY), namely 35% from irrigated rice fields, 33% from settlements, and 24% from forest/plantations. The expansion of irrigated paddy, forests/plantations and built-up areas from 2001 to 2015 decreased the ET component and slightly increased the PET component. The SW component also increased due to the expansion of irrigated paddy.

10

Also, rainfall significantly affected hydrological conditions in the Brantas watershed.

References

Abbaspour, K. (2015). SWAT-CUP Calibration and uncertainty programs. In *User Manual*. Eawag Aquatic Research. Doi: 10.1007/s00402-009-1032-4.

Ahmed, I. M., & Alla, E. M. A. (2019). Landuse impact on the environment of Tuti Island, Sudan. Geography, Environment, Sustainability. Lomonosov Moscow State University, **12**(3), pp. 27–33. doi: 10.24057/2071-9388-2018-13.

Al-Jiboori, M. H., Abu-Alshaeer, M. J., & Ahmed, M. M. (2020). Impact of land surface changes on air temperatures in Baghdad, Kuwait J. Sci. **47** (4), pp. 118 -126, 2020. Available at: http://earthexplorer.usgs.gov/ (Accessed: 12 February 2021).

Anwar, N., & Kusumawati, S. (2015). Water Allocation Optimisation for Combined Users of Energy Generation and Irrigation Demand At the Upstream Brantas River Reach Using Mixed Integer Linear Programming Method. in *International commission on irrigation and drainage*. Surabaya, pp. 4–7.

Arnold, J. G., Moriasi, D. N., Gassman, P.W., Abbaspour, K. C., White, M. J., Srinivasan, R., Santhi, C., Harmel, R. D., Van Griensven, A., Liew, M.W., Van Kannan, N., Jha, M K., Harmel, D., Member, A., Liew, M.W., Arnold, V., Jef-Frey G. (2012) Swat: Model Use, Calibration, and Validation. American Society of Agricultural and Biological Engineers. **55**(4), pp. 1491–1508.

Brighenti, T.M., Bonumá, N.B., Grison, F., Mota, A., Kobiyama, M., & Chaffe, P. (2019). Two calibration methods for modelling streamflow and suspended sediment with the swat model. *Ecological Engineering*, **127**(May 2018), pp. 103–113. doi: 10.1016/j.ecoleng.2018.11.007.

BIG (2019). Indonesia Geospatial Portal. Available at: http://tanahair.indonesia.go.id/portal-web (Accessed: 15 December 2019).

BPS Jatim(2017). *Provinsi Jawa Timur dalam Angka.* Jawa Timur Province in Figures 2017. Badan Pusat Statistik Provinsi Jawa Timur. Available at: https://jatim.bps.go.id/4dm!n/pdf%7B_%7Dpublikasi/Provinsi-Jawa-Timur-Dalam-Angka-2017.pdf (Accessed: 3 April 2020).

DLH Jatim (2017). *Dokumen Infmrasi Kinerja Pengelolaan Lingkungan Hidup Daerah Jawa Timur*. Surabaya.

Ermoshin, V., Ganzey, S., & Shiraiva, T. (2013). Land-use change in the transboundary Amur river basin in the 20th century. GEOGRAPHY, ENVIRONMENT, SUSTAINABILITY. 6(2), pp. 4–19. doi: 10.24057/2071-9388-2013-6-2-4-19.

Fitri, M., Wardoyo, W., & Theresia, S.T. (2017). Improvement Strategy of Porong Kanal Irrigation Network Performance in Delta Brantas Irrigation Area with Swot Analysis (Strength, Weakness, Opportunities, and Threats). in *The 2nd International Conference on Civil Engineering Research (ICCER) 2016 "Contribution of Civil Engineering toward Building Sustainable City"*. Surabaya, pp. 19–26. doi: 10.12962/j23546026.y2017i1.2186.

Indarto, I., Andiananta Pradana, H.,Wahyuningsih, S., & Umam, M.K..(2020). Assessment of hydrological alteration from 1996 to 2017 in Brantas watershed, East Java, Indonesia. Journal of Water and Land Development. **46(46)**, pp. 121–130. doi: 10.24425/jwld.2020.134204

IPCC (2007). Climate Change 2007: The Physical Science Basis. Contribution of Working Group I to the Fourth Assessment

Kang, Y., Gao, J., Shao, H., Zhang, Y. (2019). Quantitative Analysis of Hydrological Responses to Climate Variability and Land-Use Change in the Hilly-Gully Region of the Loess Plateau, China. Water. MDPI AG, 12(1), p. 82. Doi: 10.3390/w12010082.

Lamichhane, S., & Shakya, N. (2019). Integrated Assessment of Climate Change and Land Use Change Impacts on Hydrology in the Kathmandu Valley Watershed, Central Nepal', *Water*. MDPI AG, 11(10), p. 2059. doi: 10.3390/w11102059.

Li, F., Alewell, C., Borrelli, P., Meusburger, K., & Panagos, P. (2019). Land-use change impacts hydrology in the Nenjiang River Basin, Northeast

China. *Forests.* 10(6), pp. 1–18. doi: 10.3390/f10060476.

Li, Y., Chang, J., Luo, L., Wang, Y., Guo, A., Ma, F., Fan, J. (2019). Spatiotemporal impacts of land use land cover changes on hydrology from the mechanism perspective using SWAT model with time-varying parameters. Hydrology Research. IWA Publishing, 50(1), pp. 244–261. Doi: 10.2166/nh.2018.006.

Liu, Z., Cuo, L., Li, Q., Liu, X., Ma, X., Liang, L., & Ding, J. (2020). Impacts of Climate Change and Land Use/Cover Change on Streamflow in Beichuan River Basin in Qinghai Province, China. Water, 12(4), p. 1198. doi: 10.3390/w12041198.

Lu, Z., Zou, S., Qin, Z., Yang, Y., Xiao, H., Wei, Y., Zhang, K., & Xie, J. (2015). Hydrologic Responses to Land Use Change in the Loess Plateau: Case Study in the Upper Fenhe River Watershed. Advances in Meteorology. doi: 10.1155/2015/676030.

Marie Mireille, N., M. Mwangi, H., K. Mwangi, J., Mwangi Gathenya, J. (2019). Analysis of Land Use Change and Its Impact on the Hydrology of Kakia and Esamburmbur Sub-Watersheds of Narok County, Kenya. Hydrology. MDPI AG, 6(4), p. 86. doi: 10.3390/hydrology6040086.

Moriasi, D.N., Arnold, J.G., Liew, M.W., Van-Bingner, R. L., Harmel, R.D., & Veith, T. L. (2007). Model Evaluation Guidelines For Systematic Quantification Of Accuracy In Watershed Simulations. 50(3), pp. 885–900.

Nikitin, M. A., Tatarinovich, E.V., Rozinkina, I.A., & Andrei E. (2019). Effects of deforestation and aforestation in the central part of the East European plain on regional weather conditions. *Geography, Environment, Sustainability*. Lomonosov Moscow State University. 12(2), pp. 259–272. doi: 10.24057/2071-9388-2019-12.

Parece, T. E., & Campbell, J. B. (2015). Land Use/Land Cover Monitoring and Geospatial Technologies: An Overview. pp. 1–32. doi: 10.1007/978-3-319-14212-8_1.

Pignotti, G., Rathjens, H., Cibin, R., Chaubey, I., & Crawford, M. (2017). Comparative analysis of HRU and grid-based SWAT models. Water *(Switzerland)*, **9**(4), p. 272. doi: 10.3390/w9040272.

Ptak, M., & Ławniczak, A. E. (2012). Changes in land use in the buffer zone of lake of the Mała Wełna catchment. Limnological Review. Berlin: Sciendo, 12(1), pp. 35–44. doi: https://doi.org/10.2478/v10194-011-0043-z.

Rafiei, V., Ghahramani, A., An-Vo, D., & Mushtaq, S. (2020). Modelling Hydrological Processes and Identifying Soil Erosion Sources in a Tropical Catchment of the Great Barrier Reef Using SWAT. *Water.* 12(8), p. 2179. doi: 10.3390/w12082179.

S.L. Neitsch, J.G. Arnold, J.R. Kiniry, J. R. W. (2011). *Soil and Water Assessment Tool Theoretical Documentation Version 2009*. Texas: BLACKLAND RESEARCH CENTER ○ TEXAS AGRICULTURAL EXPERIMENT STATION.

IPCC (2007). *AR4 Climate Change 2007: The Physical Science Basis — IPCC*, *Contribution of Working Group I to the Fourth Assessment Report of the Intergovernmental Panel on Climate Change*. Available at: https://www.ipcc.ch/report/ar4/wg1/ (Accessed: 13 October 2020).

Spruce, J., Bolten, J., Srinivasan, R., Lakshmi, V. (2018). Developing Land Use Land Cover Maps for the Lower Mekong Basin to Aid Hydrologic Modeling and Basin Planning. Remote Sensing. MDPI AG. 10(12), p. 1910. doi: 10.3390/rs10121910.

Valiant, R., Nugroho, W., Bisri, M., Utomo, W. (2021). Water productivity simulation for irrigated farmlands in the Brantas River Basin. Journal of Degraded and Mining Lands Management. **8**(2), pp. 2577–2585. doi: 10.15243/jdmlm.2021.082.2577.